Monthly Notices of the ROYAL ASTRONOMICAL SOCIETY

MNRAS **509,** 1848–1853 (2022) https://doi.org/10.1093/mnras/stab3003
Advance Access publication 2021 October 20

Astrosat: forecasting satellite transits for optical astronomical observations

James Osborn [1]★ Laurence Blacketer,[2] Matthew J. Townson [1] and Ollie J. D. Farley [1]

[1]*Centre for Advanced Instrumentation, Department of Physics, Durham University, Durham DH1 3LE, UK*
[2]*Northern Space and Security, Aykley Heads Business Centre, Aykley Heads, Durham DH1 5TS, UK*

Accepted 2021 October 14. Received 2021 October 14; in original form 2021 September 8

ABSTRACT

The impact of large-scale constellations of satellites, is a concern for ground-based astronomers. In recent years there has been a significant increase in the number of satellites in low-Earth orbit and this trend is set to continue. The large number of satellites increases the probability that one will enter the field of view of a ground-based telescope at the right solar angle to appear bright enough that it can corrupt delicate measurements. We present a new tool 'Astrosat' that will project satellite orbits onto the RA/Dec. coordinate system for a given observer location and time and field of view. This enables observers to mitigate the effects of satellite trails through their images by either avoiding the intersection, post-processing using the information as a prior or shuttering the observation for the duration of the transit. We also provide some analysis on the apparent brightness of the largest of the constellations, Starlink, as seen by a typical observatory and as seen with the naked eye. We show that a naked eye observer can typically expect to see a maximum of 5 Starlink satellites at astronomical twilight, when the sky is dark. With the intended 40 000 satellites in the constellation that number would increase to 30.

Key words: light pollution – methods: analytical – methods: observational – site testing – space vehicles.

1 INTRODUCTION

The effect of the increasingly numerous satellite constellations on ground-based astronomy is an area of significant and timely concern for astronomers (see e.g. Hainaut & Williams 2020; McDowell 2020; Tyson et al. 2020; Vera Rubin Observatory Project Science team 2020; Bassa, Hainaut & Galadi-Enriquez 2021; Williams et al. 2021). As a satellite transits through the field of view of the telescope an artefact can be imprinted into the scientific data, for example a bright streak across an image. In the worst case these artefacts can lead to the data being unusable. Therefore, there is a demand for new astronomical tools which will support astronomers in mitigating these detrimental effects.

Several tools exist which can be used to find the position of a particular satellite. However, in order to mitigate the deleterious effects, astronomers need to know which satellites will intersect with a given part of the sky. Here, we present a new PYTHON tool, Astrosat[1], which calculates which satellites can be seen by a given observer in a given field of view at a given observation time and observation duration. This includes the geometry of the satellite and observer but we also estimate the expected apparent brightness of the satellite to aid astronomers in assessing the impact on their observations.

This tool could be used by several communities. Astronomers can use the tool to mitigate the effects of satellites on their scientific observations. This could be accomplished by scheduling observations to minimize the brightest satellite transits, developing active shuttering capabilities to block the short transit duration in real time, or as a prior for post-processing techniques to identify the trails in raw data (Hainaut & Williams 2020). Landscape and astro-photographers can likewise use the tool to plan their activities in order to avoid or even include the satellite trails depending on their desired impact. The tool could also be used for outreach activities to visualize and demonstrate the effect of the satellites on scientific observations but also how our naked-eye view of the night-sky is being impacted (Venkatesan et al. 2020). Astrosat is based on a central API which can be easily scripted into stand-alone tools or integrated into other software pipelines.

2 ASTROSAT

2.1 Orbit modelling

The space object orbits are generated using the Simple General Perturbations 4 (SGP4) orbital propagator together with Two Line Element (TLE) sets acquired from Celestrak compiled by T.S. Kelso.[2] Here, we use TLEs for all active satellites (4633 satellites at the time of writing) and for the brightest objects (164 objects), including for example, rocket bodies.

A TLE, which is two lines of 69 characters describing the orbit of a space object at a particular instant in time, is generated by fitting an SGP4-generated orbit to the result of an orbit determination process applied to a series of observations of a space object. The best-fitting orbital elements, and the epoch at which they are valid, are then encoded into the two lines of the TLE (Vallado et al. 2006).

★ E-mail: james.osborn@durham.ac.uk
[1]https://github.com/james-m-osborn/astrosat
[2]https://celestrak.com/

Because SGP4 is an analytical technique that uses simplified force modelling, and the numerical precision is limited to two lines of 69 characters, the positional accuracy of a TLE is also limited. However, it is not possible to quantify the accuracy of any individual TLE as it depends on the accuracy of the underlying observations, which are unknown. The positional uncertainty in a TLE of a large well-tracked space object is thought to be on the order of a few km, primarily in the in-track direction (Vallado & Cefola 2012). This uncertainty increases further as the position is propagated away from TLE epoch using SGP4.

The accuracy requirements for assessing the time at which a space object will transit the field of view will depend on the size of the field, the length of the exposure and the apparent angular velocity of the object.

If the TLEs are up to date (they are updated several times a day but the exact update rate of celestrak is unknown), then a worst-case estimate can be found by converting the expected orbital error into an angular or temporal error.

For the in-track error, it is the associated temporal error that is important. The object will still pass through the field but at a different time than expected. The worst case is a low-altitude orbit viewed at zenith when the space object will have the largest apparent angular velocity. Assuming circular orbits, the apparent angular velocity can be calculated using

$$v = \frac{\sqrt{GM_E/(r + R_E)}}{z}, \tag{1}$$

where G is the gravitational constant, $M_{\rm E}$ is the mass of the Earth, $R_{\rm E}$ is the radius of the Earth, r is the altitude of the object, and z is the range to the object from the observer.

If we assume an object orbiting in a low orbit at 335 km, then a 2 km in-track error (Vallado & Cefola 2012) will convert to 0.35 deg or 0.27 s. This will reduce for higher altitude orbits and lower elevations but increase significantly for out of date TLEs. For example an in-track error of 25 km (Vallado & Cefola 2012) will lead to an angular offset of 4.3 deg or 3.26 s. To mitigate this error we list satellites with an expected intersection at +/− 5 s of the observation time such that all objects are listed. Therefore, due to the precision of the TLEs, it should be noted that precise time estimates are not possible. Despite the large component of TLE uncertainty in the in-track direction, early TLEs can still provide useful information on the intersections between the field and a space object orbit, if not the precise time of transit.

The cross-track error is more critical as it determines whether the object will pass through the field or not. The expected precision in the cross-track direction is better with values of a few hundred metres generally quoted (Vallado & Cefola 2012). If we assume a cross-track error of 500 m then the expected angular error for a low altitude object (335 km) at zenith (worst case) is 0.09 deg (5.2 arcmin). This is difficult to mitigate and will have a larger real effect on smaller fields. The field of view could be expanded by this distance and the results interpreted probabilistically.

It is recommended that the tool is run as close as possible to the planned observation to ensure the highest possible accuracy. The TLEs are archived so can be used for post-processing at a later date without any loss of precision.

2.2 Brightness modelling

Not all satellite transits impact astronomical observations. For the satellite transit to be an issue it needs to have a significant number of photons to affect the analysis of the astronomical target. Hence, it is important to not only know details of when and where a transit occurs, it is also important to know the expected brightness of the transiting satellite. It is also worth pointing out that all attempts at estimating the expected apparent brightness of a satellite require assumptions on the size, orientation, and specularity of the satellite, all of which are often unknown.

The apparent brightness of the satellite can be approximated by (McCue, Williams & Morford 1971)

$$m = -26.74 - 2.5\log_{10}\left(\frac{A\gamma f(\phi)}{z^2}\right) + x\chi, \tag{2}$$

where A is the cross-sectional area, γ is the albedo or reflectivity, ϕ is the solar phase angle, f is a function that defines the fraction of reflected light based on the solar phase angle, z is the range to the satellite from the observer, x is the atmospheric absorption coefficient, 0.12 mag/airmass in the V band (Patat et al. 2011; Hainaut & Williams 2020) and χ is the airmass. Generally, for elevation angles, ϵ, greater than 10 deg from the horizon a simple $\chi = 1/\cos(\pi/2 - \epsilon)$ can be used. However, for low elevation angles, which can be the case for satellites, we need to include the curvature of the Earth. Here, we estimate the airmass directly from the range to the object and orbital altitude of the object.

We can assume a diffuse spherical model for the satellite, in which case the function, f is given by (McCue et al. 1971)

$$f(\phi)_{\rm diff\_sphere} = \frac{2}{3\pi}\left((\pi - \phi)\cos\phi + \sin\phi\right). \tag{3}$$

In recent publications, it has been demonstrated that Starlink satellites show very little dependence on the solar phase angle (see e.g. Horiuchi, Hanayama & Ohishi 2020). In Astrosat, it is possible to use a diffuse spherical model or to set $f(\phi) = 1$. In this study, we use $f(\phi) = 1$ for starlink satellites.

This is obviously a very rough approximation. We need to assume a cross-sectional area and reflectivity coefficient for each satellite. As these are not known, we assume a circular cross-section with a radius of 1 m and $\gamma = 0.25$. These values are thought to be representative of the Starlink-like satellites (Hainaut & Williams 2020).

Recent measurements of the new generation of Starlink visorsat satellites suggest that the V magnitude has been reduced by 1.3 mag (Mallama 2021). Therefore, here we reduce the albedo by 30 per cent to reflect this.

In Astrosat, the reflection cross-section can be provided by the user and therefore can be tuned as more data become available for Starlink and other satellites.

LEO constellations are likely to be the most disruptive to astronomical observations due to their low altitude and isotropic distribution. The exception to this will be rocket bodies which, although few in number, can be large and therefore appear very bright. With the growing interest in the space environment and satellite surveillance and tracking, we expect to be able to build a data base for the $A\gamma$ product for different space object and satellite types.

Currently, this model is valid for the V band. We intend to develop the model further to include a wavelength scaling and even consider the implications in the radio spectrum. This is left as an extension for the future.

The model does not include transient events, such as flares or rotating objects which are impossible to predict without a lot more information about a particular object and its dynamics.

2.3 Functionality

Astrosat is based on a central application programming interface (API) which can be easily scripted into stand-alone tools or integrated into other software pipelines.

As previously stated the space object TLEs are downloaded from Celestrak at run-time (if necessary). To validate the satellite positions we calculate the time and elevation angle at culmination for a random sample of 30 starlink satellites. That is the point of highest elevation angle as seen by an observer on the ground.

We compared the predicted satellite positions and time at culmination from Astrosat and Heavens-Above.com[3]. We find that the elevation angle agrees to within the precision listed on Heavens-Above (1 deg) in every case. The time of culmination differs by 2.6 +/− 9.2 s. It is likely that the difference is due to the two systems using different TLEs.

The position of the stars is found by querying the SIMBAD Astronomical Database[4] (Wenger et al. 2000) for fields less than 2 deg or by searching the Yale Bright Star Catalogue[5] (Hoffleit & Warren 1991) for larger fields.

To find the space objects that intersect with any given field of view, the software uses a nested search algorithm. Initially, we estimate the apparent position of every object as seen by the observer every 10 s during the observation window. For all the satellites that come within 15 deg of the target direction, we undergo a second more precise scan, probing the positions every 1 s. 15 deg is chosen as the fastest we expect an object to appear is 1.3 deg/s for an object orbiting at 335 km (Starlink lower limit) at zenith. This ensures that even the fastest objects are seen in the search radius at least once with 10 s cadence. We then interpolate between the one second position probes to estimate the exact times the object enters and exits the field of view. The location is checked at the mid-intersection time as a validation of the interpolation. The solar phase angle, if used, can be calculated using the sine rule and the shadow of the Earth is also included.

To estimate the apparent position of the stars and space objects as seen by an observer we use pyephem[6]. This is a well-used library and has been validated elsewhere. We have implemented previously published brightness estimation algorithms and these have also compared with measurements of Starlink satellites elsewhere (see Section 2.2).

As an example of benchmark run-times, we probed 0.5 deg field of views as seen from an observer at Durham, UK, for 21:00 on the 27th September 2021 for a 1-h observation. We include the current case of 1600 Starlink satellites as well as artificially generated TLEs for 12 000 and 40 000 Starlink satellites. The computer used for the benchmark tests is 2019 MacBook Pro, 2.8 GHz Quad-Core Intel Core i7 with 16GB memory. The tests took 18 s, 46 s, and 3:20 min for the 1600, 12 000, and 40 000 satellite case, respectively. These processing times are not prohibitive and could be improved with more sophisticated search algorithms.

2.4 Vega example

Fig. 1 shows an example output from the tool. In this example, the observer was in Durham, UK, the target was set to Vega with a 1 deg field at 21:00 on the 27th September 2021 for a 1-h observation.

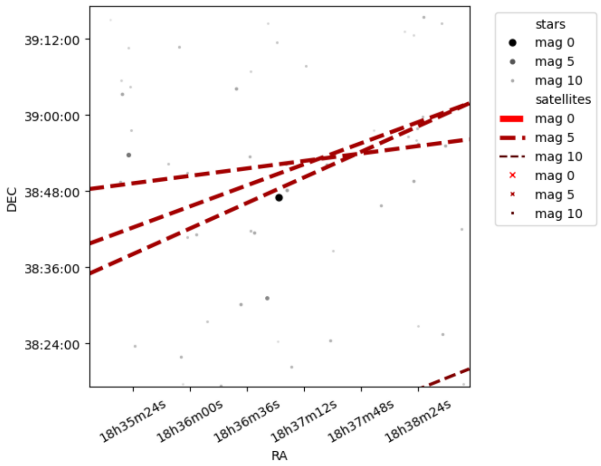

Figure 1. Example field image showing a 1 deg field of view around the star Vega. The brightness of the stars are shown by the grey-scale and size of the point. The satellite trails are shown in red dashed line with line-width and red colour intensity denoting the apparent magnitude of the satellite. The designations, time of interception, duration of transit and expected brightness of the satellites are shown in the terminal, recreated in Table 1. This example is for 21:00 on the 2021 September 27 from Durham, UK.

Table 1. Example output for satellite intersection with a 1 deg field of view around the star Vega for 21:00 with a hour observation on the 2021 September 27 as seen from Durham, UK.

Name	Time (UTC)	Duration (s)	Magnitude (*V*)
STARLINK-2231	20:09:07	1.3	5.38
STARLINK-2719	20:26:13	1.2	5.42
GLOBALSTAR M080	20:32:48	0.4	7.46
STARLINK-1293	20:37:54	1.5	5.45

The figure shows the bright star of Vega in the centre with other stars shown in black. The brightness of the star is shown by the size and brightness of the marker as indicated in the legend. The predicted satellite trails are shown in red-dashed lines with the expected brightness designated by the thickness and saturation of the line, as shown in the legend. In this case four satellite intersections are predicted at magnitudes that can be seen on this scale. The designations, time of interception, duration of transit and expected brightness of the satellites are shown in the terminal, recreated in Table 1.

3 ANALYSIS

In this section, we provide some analysis from Astrosat. We concentrate on Starlink satellites, as they are currently the most numerous constellation with plans to significantly expand. At the time of writing there are 1635 TLEs attributed to starlink satellites. This means that they have the potential to have the greatest impact on an astronomical context.

In addition to the apparent brightness of the satellite we also include the satellite density and apparent angular velocity all as a function of elevation angle. By combining these three parameters an observer can assess the effect of the satellites in terms of signal per pixel per exposure for a given system (pixel size and exposure time). This is important because it is the received flux per pixel per exposure that is important. For example a faint but slow satellite might have a great effect that a fast and bright satellite.

[3]https://www.heavens-above.com/
[4]http://simbad.u-strasbg.fr/simbad/
[5]http://tdc-www.harvard.edu/catalogs/bsc5.html
[6]https://rhodesmill.org/pyephem/

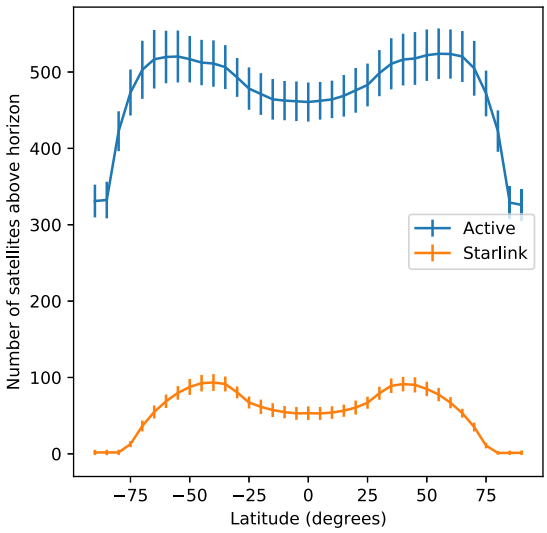

Figure 2. Number of satellites above horizon at any moment. At the poles, only polar orbits are visible, hence the lower number of satellites visible. The maximum is at approximately ±50 deg caused by the increased density of mid-inclination orbits such as Starlink. To estimate the error bars we calculate the number of satellites visible above the horizon every hour for a 24-h period. The error bars show the standard deviation of this value. This is a useful tool to demonstrate the variance of the number of visible objects at any particular time.

Unless stated otherwise the analysis is presented for a 'typical' observatory at 25 deg North (or south) in Latitude and 1000-m altitude. The longitude is set to 0 but does not matter for this analysis. This typical observatory is used for this study as the latitude of the observatory does make a difference in the number of satellites visible above the horizon.

3.1 Number density of Starlink satellites

Fig. 2 shows the total number of satellites above the horizon as a function of latitude. Considering the line for all active satellites in blue, the plot shows that approximately 330 satellites are above the horizon to an observer located at either pole. These are the high numbers of systems that are in polar orbits. For an observer located at the equator, approximately an additional 120 satellites are visible, for a total of 450. This number now includes those satellites in lower inclination orbits that were not visible to an observer at the poles. The number of satellites above the horizon peaks at approximately ±50, which results in an increased spatial density caused by mid-inclination satellites such as Starlink. The shape of this plot agrees with the work of McDowell (2020).

For astronomers, the total number of satellites in the sky is not so important. More interesting is the density of the satellites, or number per degree, and this varies as a function of elevation angle. Fig. 3 shows that a higher density of satellites is seen near the horizon, as expected.

3.2 Apparent brightness of Starlink satellites

Although it is the solar phase angle that determines the apparent brightness of a satellite for an observer, this is not very useful for astronomers. In Fig. 4, we show the expected satellite brightness as a function of sun elevation angle, as seen by the observer and relative to the horizon. We see that the apparent brightness of Starlink satellites

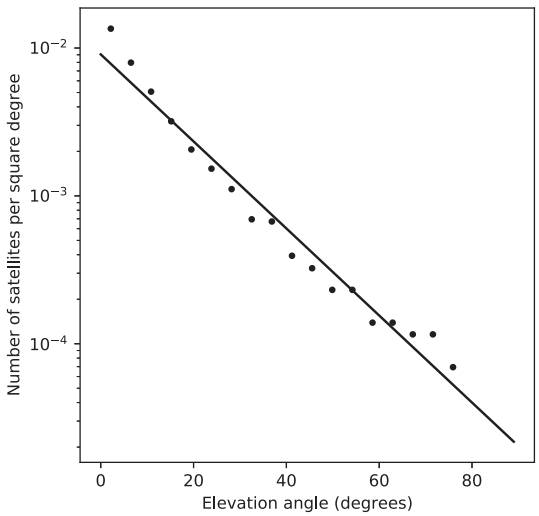

Figure 3. Number density of Starlink satellites as seen from a typical observatory at a latitude of +/− 25 deg. This is for a total number of 1635 Starlink satellites at the time of writing. The line of best fit is $y = -0.03x - 2.04$.

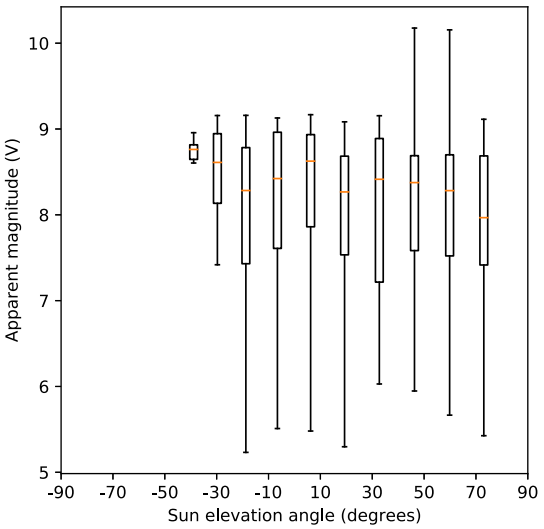

Figure 4. Apparent magnitude of Starlink satellites as a function of sun elevation (negative represents night-time when the sun is below the horizon) as seen by an observer at a typical observatory at a latitude of 25 deg North in the summer. We see that generally the Starlink satellites have an apparent magnitude of approximately 8. As the sun elevation becomes more negative the brighter satellites are not seen. Brighter satellites tend to be in lower orbits and so are lost to the Earth's shadow sooner than the higher altitude, fainter satellites. The large whiskers show the variability in the estimates which is mainly due to the variable satellite range. The central horizontal line indicates the median, the box indicates the interquartile range and the whiskers indicate the full range.

is insensitive to sun elevation angle through the day and reduces during the night, when the sun is below ∼15 deg below the horizon. This explains why satellites are generally observed at twilight, when the sky is sufficiently dark but the satellites are still sufficiently bright, maximizing the signal-to-noise ratio. The satellite brightness also has a dependence on the observation elevation angle due to the airmass dependent atmospheric extinction (see equation 2).

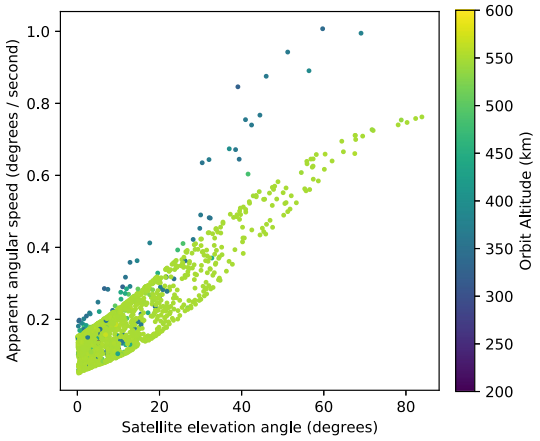

Figure 5. Angular speed of Starlink satellites as seen by an observer in a typical observatory at 25 deg North. There are two distinct sets of objects visible. The majority of Starlink satellites follow a curve from approximately 0.1 deg per second at the horizon up to approximately 0.8 deg per second at zenith. These correspond to the satellites orbiting at approximately 550 km. The scatter of the apparent angular speed is due to the projection effect determined by the relative direction of the satellite with respect to the position of the observer. There is another smaller set of faster satellites that correspond to lower orbits.

3.3 Apparent angular velocity of Starlink satellites

In order to estimate the impact on astronomy we need to be able to assess the received flux per pixel per exposure. In addition to the number density and apparent brightness of the satellite, this requires some knowledge of the apparent velocity of the satellites. Fig. 5 shows the expected apparent angular velocity of the Starlink satellites as a function of elevation angle. At low elevation angles, projection effects lead to a reduced apparent angular velocity, with maximum angular velocity at zenith. The majority of Starlink satellites follow a curve from approximately 0.1 deg per second at the horizon up to approximately 0.8 deg per second at zenith. This main branch is attributed to satellites in operational orbits near to 550 km. Another branch can be seen corresponding to lower altitude and hence apparently faster satellites. These are satellites that are operating at lower altitudes, have recently been deployed into parking orbits, are in the process of orbit-raising, are in the process of de-orbiting or have failed.

4 PROJECTION TO THE FUTURE

There is considerable interest in the impact of future satellite constellations on astronomy and also on the naked eye visibility of the night sky. Using this model we can predict future satellite density and brightness based on projected constellation orbits and numbers. We define orbital parameters for a potential Starlink like constellation from the ASTRON package (Bassa et al. 2021).

Fig. 6 shows examples of the current and future maps of naked eye visible satellites at a very dark site (<magnitude 6) at the end of astronomical twilight (sun is 18 deg below the horizon). This is a worst-case model. This is only valid for the very best sites with no light pollution and observers with very good eyesight. Also, later in the night there is a lack of bright satellites due to the observer – satellite – sun geometry and earlier in the night the increased sky brightness will reduce the brightness limit meaning fewer satellites can be seen.

There is no difference in the relative brightness distributions but the numbers of visible satellites increases dramatically. The figures shows that the expected number of visible satellites during twilight (i.e. the maximum number) goes from approximately 5 for 1600 satellites, to 10 and 30 for 12 000 and 40 000 satellites, respectively.

This does rely on our brightness model being statistically accurate.

5 CONCLUSIONS

We present a new software tool, Astrosat, written in PYTHON and available at https://github.com/james-m-osborn/astrosat. Astrosat is based on a central API which can be easily scripted into stand-alone tools or integrated into other software pipelines.

Astrosat allows users to probe expected satellite/space object transit events through a given field of view for any observer location, time, field of view and observation duration. Astrosat can be used as an API which can be integrated into existing pipelines or as a stand-alone tool. We expect astronomers will be able to use the tool to schedule observations to minimize satellite impact, to shutter transit

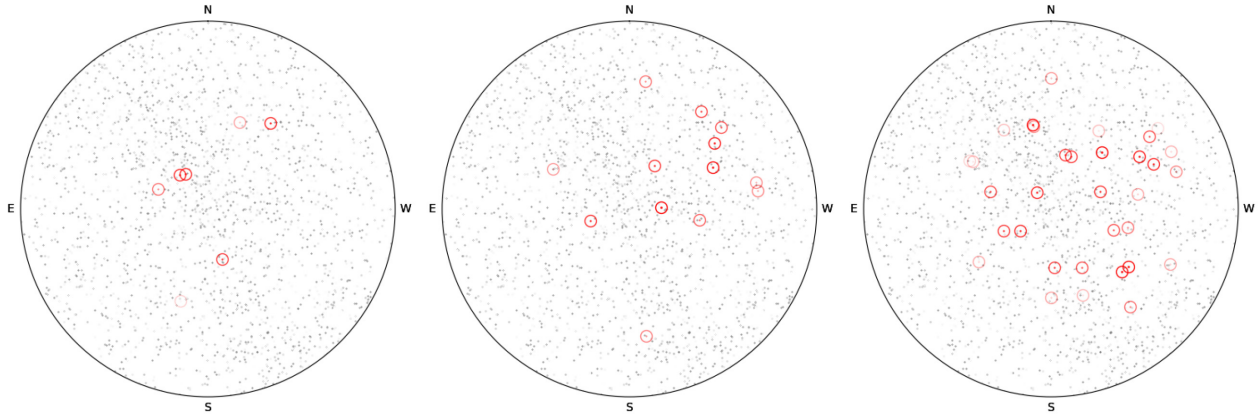

Figure 6. Example satellite visibility map down to magnitude 6 in the *V* band (naked eye limit at a very dark site) for an observer at 25 deg North. The time is selected such that the sun is at 18 deg below the horizon, classified as astronomically dark. Stars are shown in black and satellites in red and are highlighted by circle to increase visibility. From left to right we show the naked eye visibility of an example LEO satellite constellation with 1600 satellites (left, current Starlink situation, 7 visible satellites), 12 000 satellites (centre, approved Starlink plan by the US Federal Communications Commission, 13 visible satellites) and 40 000 (right, planned Starlink constellation, 31 visible satellites).

events or to identify artefacts in data by using the expected transits as a prior in data analysis pipelines. In addition, landscape and astrophotographers can use the tool to plan their activities in order to avoid or even include the satellite trails depending on their desired impact. The tool can also be used for outreach activities to visualize and demonstrate the effect of the satellites on scientific observations but also how our naked-eye view of the night sky is being impacted.

We have presented basic analysis such that astronomers can assess the expected impact of Starlink and similar satellite constellations. We have shown the expected number, apparent brightness, and angular speed of the satellites all as a function of elevation angle.

As expected, more satellites can be seen at lower elevation angles due to the projection effect. For the same reason, these satellites also appear to move more slowly (∼0.1 degrees per second near the horizon compared to ∼0.8 degrees per second at zenith).

Interestingly satellites tend to have a consistent brightness during the daytime and become fainter at night as they move into the shadow of the Earth. However, they are most visible during twilight when they still have the same apparent brightness but the background from the sky is significantly reduced. The brighter satellites tend to be seen at higher zenith angles and occur at twilight when the angle subtended between the sun, satellite and observer is optimal.

In addition we also show example visualizations of the night sky at twilight for 1600 (current number of Starlink satellites), 12 000 (number of authorized Starlink satellites) and 40 000 (number of planned Starlink satellites). We expect a naked-eye observer will be able to see a maximum of approximately 5, 10, and 30 satellites during the twilight period for each scenario, respectively.

ACKNOWLEDGEMENTS

JO acknowledges the UK Research and Innovation Future Leaders Fellowship (MR/S035338/1) and the Science and Technology Facilities Council (STFC) through grant ST/P000541/1.

This research has made use of the SIMBAD database, operated at CDS, Strasbourg, France.

The authorsthank T.S. Kelso for maintianing the TLE database.

The simulations in this paper make use of the NUMPY (Van der walt, Colbert & Gaël 2011), SCIPY (Virtanen et al. 2020), AOTOOLS (Townson et al. 2019), and MATPLOTLIB (Hunter 2007) PYTHON packages.

We would like to thank the reviewer, Dr. Hainaut, whose insightful comments certainly improved this paper and helped to make astrosat more complete.

DATA AVAILABILITY

No data were archived for this publication. Data for plots can be generated using Astrosat.

REFERENCES

Bassa C. G., Hainaut O. R., Galadi-Enriquez D., 2021, A&A, preprint (arXiv: 2108.12335)
Hainaut O. R., Williams A. P., 2020, A&A, 636, A121
Hoffleit D., Warren W., Jr, 1991, ADC Selected Astronomical Catalogs, 1, Astronomical Data Center, NSSDC/ADC
Horiuchi T., Hanayama H., Ohishi M., 2020, ApJ, 905, 3
Hunter J. D., 2007, Comput. Sci. Eng., 9, 90
Mallama A., 2021, preprint (arXiv:2101.00374)
McCue G. A., Williams J. G., Morford J. M., 1971, Planet. Space Sci., 19, 851
McDowell J. C., 2020, ApJ, 892, L36
Patat F. et al., 2011, A&A, 527, A91
Townson M. J., Farley O. J. D., Orban de Xivry G., Osborn J., Reeves A. P., 2019, Opt. Express, 27, 31316
Tyson J. A. et al., 2020, AJ, 160, 226
Vallado D., Cefola P., 2012, Proc. Int. Astronaut. Cong., 7, 5812
Vallado D., Crawford P., Hujsak R., Kelso T., 2006, Revisiting Spacetrack Report #3: Rev 1. AIAA/AAS Astrodynamics Specialist Conference and Exhibit, Keystone, Colorado
Van der walt S., Colbert S. C., Gaël V., 2011, Comput. Sci. Eng., 13, 22
Venkatesan A., Lowenthal J., Prem P., Vidaurri M., 2020, Nat. Astron., 4, 1043
Vera Rubin Observatory Project Science Team, 2020, Technical Report, Impact on Optical Astronomy of LEO Satellite Constellations, Document-33805. Rubin Observatory
Virtanen P. et al., 2020, Nat. Methods, 17, 261
Wenger M. et al., 2000, A&AS, 143, 9
Williams A., Hainaut O., Otarola A., Tan G. H., Biggs A., Phillips N., Rotola G., 2021, Technical Report, A Report to ESO Council on the Impact of Satellite Constellations. ESO, München, Germany

This paper has been typeset from a TEX/LATEX file prepared by the author.